

# ChemComm

This article is part of the

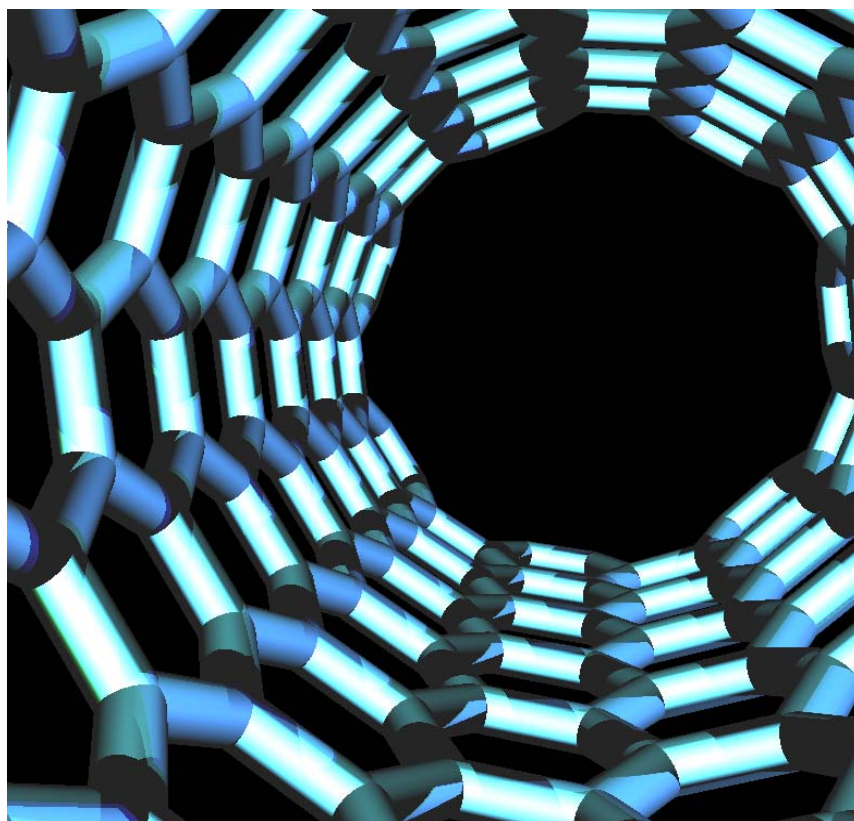
## Carbon Nanostructures web themed issue

This issue showcases high quality research in the field of nanotechnology,  
specifically research that deals with carbon nanostructures

**Guest Editors:** Professors Nazario Martín, Dirk Guldi and Luis Echegoyen

Please visit the website to access the other articles in this issue:-

<http://www.rsc.org/chemcomm/carbonnanostructures>



# Diameter-dependent, progressive alkylcarboxylation of single-walled carbon nanotubes†

Shunliu Deng,<sup>ab</sup> Alexandra H. Brozena,<sup>a</sup> Yin Zhang,<sup>ac</sup> Yanmei Piao<sup>a</sup> and YuHuang Wang<sup>\*ad</sup>

Received 15th September 2010, Accepted 21st October 2010

DOI: 10.1039/c0cc03896b

We demonstrate diameter-dependent, progressive alkylcarboxylation of single-walled carbon nanotubes by recycling a modified Billups–Birch reaction. The strong diameter dependence was confirmed by Raman spectroscopy. Alkylcarboxylation made SWNTs soluble in water, allowing the more readily functionalized, smaller diameter nanotubes to be enriched by water extraction.

Single-walled carbon nanotubes (SWNTs) exhibit interesting electrical and optical properties that are sensitively dependent on their structure.<sup>1</sup> The bandgap of a semiconducting nanotube, for example, is inversely proportional to the nanotube diameter. The existence of a large number of different structures in as-synthesized samples poses a significant technical challenge to the use of SWNTs in potential applications including optoelectronics and sensors. However, the rich SWNT structures have also opened opportunities to advance fundamental understanding of chemical reactivity and selectivity in carbon materials.<sup>2</sup>

We report a diameter-dependent, alkylcarboxylation reaction of SWNTs by adapting the Billups–Birch reductive alkylation<sup>3</sup> in a recycling procedure. This alkylcarboxylation chemistry allowed us to functionalize HiPco SWNTs progressively from the smaller diameter nanotubes towards the larger ones. The addition of alkylcarboxylic acid functional groups to the carbon lattice made SWNTs soluble in water. The diameter-dependent reactivity selectively enhanced the water solubility of smaller diameter tubes, allowing for their separation by a competitive water–hexane partitioning method to divide the functionalized sample into different aqueous extracts of decreasing functionalization and solubility, yet also increasing diameter. The results were characterized with Raman spectroscopy which allowed us to identify diameter range characteristics of the functionalized SWNT fractions.

In a typical reaction, HiPco SWNTs (provided by Rice University, batch 112.1) were first purified using a H<sub>2</sub>O<sub>2</sub>/HCl one-pot purification method as previously reported<sup>4</sup> to remove catalytic iron particles and amorphous carbon. The reaction began by exfoliating 0.050 g (4.17 mmol of carbon) of the purified HiPco SWNTs in 75 mL liquid ammonia with the

addition of sodium (0.145 g, 6.30 mmol). To the homogeneous dispersion was then added 6-bromohexanoic acid (1.625 g, 8.3 mmol) and the mixture was allowed to react for one hour. The nanotubes were repeatedly functionalized by alternately adding sodium and 6-bromohexanoic acid to the mixture to yield *N*-SWNT-[(CH<sub>2</sub>)<sub>5</sub>COONa]<sub>x</sub> (*N* indicates the number of reaction cycles). This recycling experimental protocol has allowed us to functionalize SWNTs with ω-bromocarboxylic acids to produce water soluble nanotubes (up to 3380 mg L<sup>-1</sup>), approaching the solubility recently achieved only with chlorosulfonic super-acid.<sup>5</sup>

This progressive, functionalization chemistry shows a clear reactive preference for smaller diameter SWNTs as revealed by following the product using resonant Raman spectroscopy after each reaction cycle. The covalent addition of -(CH<sub>2</sub>)<sub>5</sub>COOH onto the lattice of a SWNT depresses its characteristic Raman radial breathing mode (RBM, ~100–400 cm<sup>-1</sup>) due to reduced tubular symmetry. The RBM peak frequency is inversely proportional to the

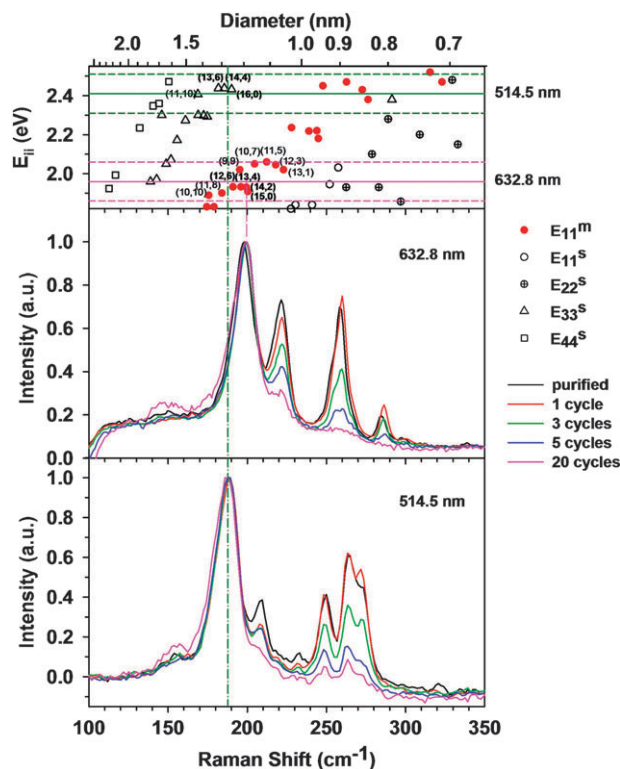


**Fig. 1** The evolution of diameter-dependent alkylcarboxylation monitored by Raman spectroscopy. The Raman spectra were normalized to the RBM peak with the highest intensity. The corresponding Kataura plot is shown in the top panel with the excitation windows indicated for 632.8 and 514.5 nm excitation lines, respectively.

<sup>a</sup> Department of Chemistry and Biochemistry, University of Maryland, College Park, MD 20742, USA. E-mail: yhw@umd.edu; Fax: +1-301-314-9121; Tel: +1-301-405-3368

<sup>b</sup> Department of Chemistry, Xiamen University, Xiamen, China

<sup>c</sup> Department of Physics, Xi'an JiaoTong University, Xi'an, China

<sup>d</sup> Maryland NanoCenter, University of Maryland, College Park, MD 20742, USA

† This article is part of the 'Carbon Nanostructures' web-theme issue for ChemComm.

corresponding SWNT diameter.<sup>6</sup> A clear diameter selectivity associated with the formation of  $N$ -SWNT- $[(\text{CH}_2)_5\text{COONa}]_x$  can be deduced from the Raman spectra. As shown in Fig. 1, the RBMs of the purified starting SWNT materials exhibit four typical peaks (198, 221, 258 and 285  $\text{cm}^{-1}$ ) in the resonance window of the 632.8 nm excitation line. As the reaction was repeated, the RBM peaks of the smaller diameter SWNTs (221, 258 and 285  $\text{cm}^{-1}$ ) decreased continuously and almost completely diminished after 20 cycles of reaction, when only the peaks at 198 and 221  $\text{cm}^{-1}$  were still observed. These trends suggest that the alkylcarboxylation of HiPco SWNTs prefers smaller diameter nanotubes. The diameter dependence was confirmed by the Raman results obtained with both 632.8 nm and 514.5 nm excitation (Fig. 1). Since these two excitation lines are in resonance with metallic and semiconducting SWNTs of similar diameters respectively, the diminishing smaller diameter nanotubes in both excitation windows suggest this alkylcarboxylation reaction is not strongly inclined to a particular electronic type.

We attribute this diameter-dependent alkylcarboxylation reaction to diameter-dependent electron-transfer kinetics. In the Billups–Birch reaction, solvated electrons are involved in charge transfer to SWNTs. The reduction potential of  $\text{Na}^+/\text{Na}$  (in liquid ammonia) is  $-1.89$  V, lower than that of the largest semiconductor<sup>1,2</sup> and metallic<sup>7</sup> tubes within the HiPco diameter range.<sup>8</sup> Thus in the Billups–Birch reduction, CNTs act as an electron acceptor. The relative position of the Fermi level has been found to vary linearly with inverse nanotube diameter regardless of the electronic type.<sup>9</sup> Therefore, the difference in reduction potential between solvated electrons and smaller diameter/larger bandgap SWNTs is greater than that of larger diameter/smaller bandgap SWNTs. The smaller the diameter, the higher the reduction potential.<sup>2,12</sup> Thus, it is not surprising that smaller diameter carbon nanotubes render more efficient reduction in the Billups–Birch reaction.

This diameter dependence is consistent with Wunderlich *et al.*'s observation for nanotube alkylation,<sup>10</sup> but the dependence is more substantial with our recycling alkylcarboxylation method. Importantly, alkylcarboxylation enables water solubility, which has prompted us to attempt to separate the functionalized nanotubes by diameter. Wet chemistry is an attractive approach to this problem due to the prospect of high scalability. Diameter selective reactions by various functionalization methods, *e.g.* ozonolysis,<sup>11</sup> have been explored. However, successful separation is often limited due to the lack of solubility, scalability and the destructive nature of covalent methods. The current approach may overcome some of these limitations because (1) there is a strong diameter-dependent reactivity; (2) water solubility provides a means of physically separating SWNTs; (3) the Billups–Birch reaction is homogeneous which promises high scalability.

To investigate the prospect of this approach for diameter-dependent separation, we further applied a competitive solvation and partitioning technique that we developed recently<sup>12</sup> to separate functionalized SWNTs by solubility. This separation approach is depicted in Fig. 2A. The  $N$ -SWNT- $[(\text{CH}_2)_5\text{COONa}]_x$  were extracted with hexane by first re-dispersing the sample in 40 mL basic water (pH = 10). The dispersion was transferred to a separatory funnel, to which

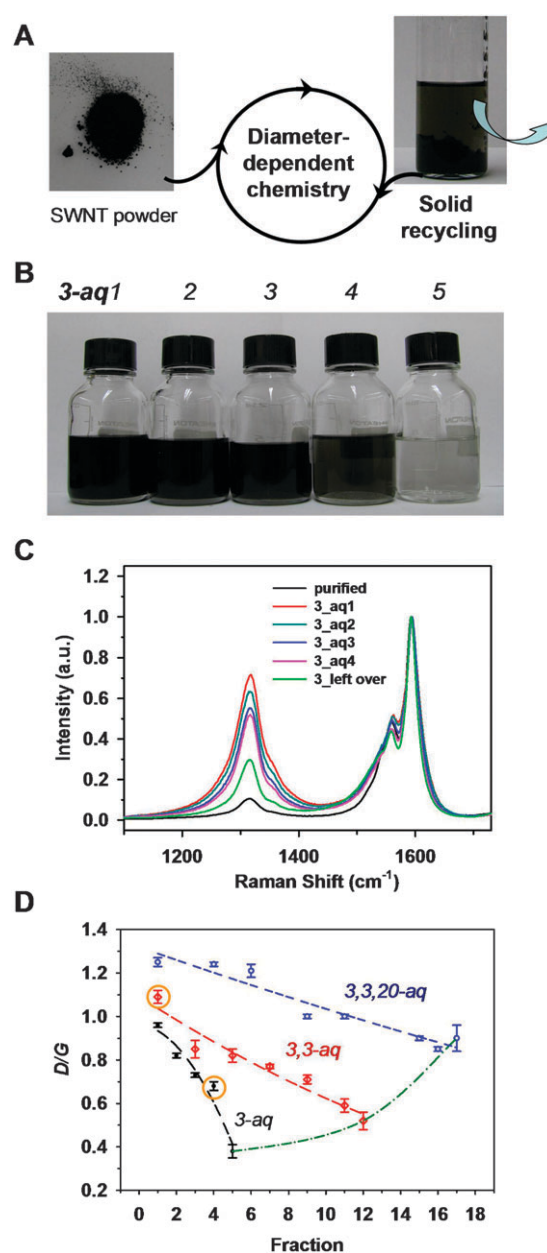


**Fig. 2** Solubility dependent water extraction of  $N$ -SWNT- $[(\text{CH}_2)_5\text{COONa}]_x$ . (A) Scheme of progressive alkylcarboxylation extraction, (B) photographs and (C) Raman spectra of water soluble fractions after 3 reaction cycles, and (D) evolution of Raman D/G peak area ratios for water soluble fractions after up to 3 + 3 + 20 reaction cycles. The Raman excitation line was 632.8 nm.

10 mL hexane was added and the mixture was shaken vigorously by hand. After phase separation, the black colored aqueous layer containing water soluble carbon nanotubes was collected, while the nanotubes remaining in the hexane layer were collected as a black solid by filtering the mixture over a Millipore TMTP membrane with 5  $\mu\text{m}$  ion-etched pores. The dispersion and extraction process was repeated with the left-over solid ( $N$ -SWNT- $[(\text{CH}_2)_5\text{COONa}]_x$ -leftover) until the aqueous layer became colorless or light colored, indicative of the separation of all the water soluble components. For sample 3-SWNT- $[(\text{CH}_2)_5\text{COONa}]_x$ , four aqueous fractions, namely 3-aq(1–4),

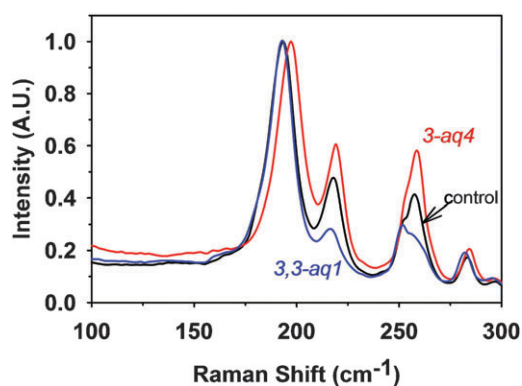


**Fig. 3** Raman spectra of nanotube fractions in comparison with the starting material. The samples were annealed at identical conditions. The laser excitation line was 632.8 nm.

were obtained (Fig. 2B). The amount of nanotubes solubilized in water was 20% of the total products. The insoluble residue was dried overnight in a vacuum oven at 80 °C and used as the starting material for an additional 3 alkylcarboxylation cycles (3,3-SWNT-[(CH<sub>2</sub>)<sub>5</sub>COONa]<sub>x</sub>). A total of 11 soluble fractions, 3,3-aq(1–11), were collected by repeated hexane extraction which was 31% of the total product. The residual insoluble solid was further functionalized for 20 cycles to yield 3,3,20-SWNT-[(CH<sub>2</sub>)<sub>5</sub>COONa]<sub>x</sub>, followed by the repeated extraction with hexane, from which a total of 5 water soluble fractions were obtained. These SWNT aqueous solutions are stable; no precipitation was observed, even after four months.

As shown in Fig. 2C and D, the Raman integrated intensity of the D and G peaks (D/G), indicative of functionalization degree of the separated water soluble carbon nanotubes, was considerably higher than both the starting material and the residual, insoluble solid. The Raman D/G of different fractions was inversely related to the order of extraction; the first extracted SWNTs exhibit the highest D/G value. This trend persisted in every extraction experiment (Fig. 2D). This is not surprising since water solubility is approximately proportional to the degree of alkylcarboxylation. Therefore, the extractions were driven by the degree of functionalization. As the extraction experiments were conducted, carbon nanotubes with different degrees of functionalization were sequentially obtained in each aqueous fraction. For example, the Raman D/G varied from 1.09 to 0.59 for the carbon nanotube contents fractionalized from 3,3-SWNT-[(CH<sub>2</sub>)<sub>5</sub>COONa]<sub>x</sub>.

In order to confirm the diameter-dependent separation, the separated soluble fractions, 3-aq4 and 3,3-aq1, were thermally de-functionalized to recover tubular structure for Raman RBM assignment. Thermal annealing took place in a 25 mm diameter quartz tube furnace under flowing Ar/H<sub>2</sub>. The temperature was raised to 100 °C and kept for 1 hour, followed by ramping at a rate of 20 °C per min up to 600 °C. The sample was kept at 600 °C for 1 hour and then allowed to cool to room temperature over 1.5 hours. Fig. 3 shows the RBM Raman spectra after thermal de-functionalization. For 3-aq4, the peak intensities at

221 and 258 cm<sup>-1</sup> increase, which suggests an enrichment of smaller diameter nanotubes in this fraction after annealing in comparison to the starting material. The next 3 cycles of functionalization were reacted with the remaining nanotubes in the 3-SWNT-[(CH<sub>2</sub>)<sub>5</sub>COONa]<sub>x</sub>-leftover material which have larger diameters than the previously extracted aqueous fractions. Consequently, 3,3-aq1 had a higher content of larger diameter nanotubes as evidenced by the diminished RBM peaks at 221 and 258 cm<sup>-1</sup>, indicative of smaller diameters (Fig. 3). These results confirm that the recycling alkylcarboxylation will selectively functionalize SWNTs in a manner that allows higher functionalized, more soluble, smaller diameter nanotubes to be extracted in earlier aqueous fractions with diameter distributions increasing for latter fractions. This type of selective partitioning of SWNTs by diameter may enable a chemical approach to carbon nanotube separation.

This work was supported by startup funds from the University of Maryland, a Doctoral New Investigator Award from the ACS Petroleum Research Fund, and a Nano-Biotechnology Initiative Start-up Award from the Maryland Department of Business and Economic Development. S.L.D. and Y.Z. acknowledge the State Scholarship Council of China for a Postdoctoral Fellowship and a Visiting Graduate Fellowship, respectively. A.H.B. acknowledges the support provided by the Department of Energy Office of Science Graduate Fellowship. S.L.D. acknowledges FPNSFC (2009J05034) for additional funding support. We thank Professor Michael Fuhrer for access to the annealing set-up.

## Notes and references

- 1 M. C. Hersam, *Nat. Nanotechnol.*, 2008, **3**, 387–394.
- 2 N. Karousis, N. Tagmatarchis and D. Tasis, *Chem. Rev.*, 2010, **110**, 5366–5397.
- 3 F. Liang, A. K. Sadana, A. Peera, J. Chattopadhyay, Z. N. Gu, R. H. Hauge and W. E. Billups, *Nano Lett.*, 2004, **4**, 1257–1260.
- 4 Y. Wang, H. Shan, R. H. Hauge, M. Pasquali and R. E. Smalley, *J. Phys. Chem. B*, 2007, **111**, 1249–1252.
- 5 V. A. Davis, A. N. G. Parra-Vasquez, M. J. Green, P. K. Rai, N. Behabtu, V. Prieto, R. D. Booker, J. Schmidt, E. Kesselman, W. Zhou, H. Fan, W. W. Adams, R. H. Hauge, J. E. Fischer, Y. Cohen, Y. Talmon, R. E. Smalley and M. Pasquali, *Nat. Nanotechnol.*, 2009, **4**, 830–834.
- 6 S. M. Bachilo, M. S. Strano, C. Kittrell, R. H. Hauge, R. E. Smalley and R. B. Weisman, *Science*, 2002, **298**, 2361–2366.
- 7 K. Murakoshi and K. Okazaki, *Electrochim. Acta*, 2005, **50**, 3069–3075.
- 8 P. Nikolaev, M. J. Bronikowski, R. K. Bradley, F. Rohmund, D. T. Colbert, K. A. Smith and R. E. Smalley, *Chem. Phys. Lett.*, 1999, **313**, 91–97.
- 9 M. J. O’Connell, E. E. Eibergen and S. K. Doorn, *Nat. Mater.*, 2005, **4**, 412–418.
- 10 D. Wunderlich, F. Hauke and A. Hirsch, *J. Mater. Chem.*, 2008, **18**, 1493–1497.
- 11 S. Banerjee and S. S. Wong, *J. Phys. Chem. B*, 2002, **106**, 12144–12151.
- 12 A. H. Brozena, J. Moskowitz, B. Y. Shao, S. L. Deng, H. W. Liao, K. J. Gaskell and Y. H. Wang, *J. Am. Chem. Soc.*, 2010, **132**, 3932–3938.